

CONFERENCES AND SYMPOSIA

PACS number: 01.10.Fv

Scientific session of the Physical Sciences Division of the Russian Academy of Sciences (25 April 2007)

A scientific session of the Physical Sciences Division of the Russian Academy of Sciences (RAS) was held on April 25, 2007 in the Conference Hall of the P N Lebedev Physical Institute, RAS. The following reports were presented at the session.

(1) **Novikov I D, Kardashev N S, Shatskii A A** (Astro-Cosmic Center, P N Lebedev Physical Institute, RAS, Moscow) "The multicomponent Universe and the astrophysics of wormholes";

(2) **Lukash V N, Mikheeva E V** (Astro-Cosmic Center, P N Lebedev Physical Institute, RAS, Moscow) "Dark matter: from initial conditions to structure formation in the Universe".

An bridged version of these reports is given below.

PACS numbers: **04.20.–q**, **04.70.–s**, **98.80.–k**
DOI: 10.1070/PU2007v050n09ABEH006381

The multicomponent Universe and the astrophysics of wormholes

I D Novikov, N S Kardashev, A A Shatskii

1. Introduction

Solutions to the pressing problems of astrophysics may prove to be paradoxical and strange from the viewpoint of current scientific dogmas.

Astrophysics (cosmology, in particular) has seen many unusual discoveries. Here is a short history of the wormhole problem in astrophysics.

The paper by Einstein and Rosen [1] published in 1935 may be considered the first serious work on wormholes. To describe a hypothetical object, they introduced a "mathematical representation of physical space by a space of two identical sheets connected by a *bridge*" [1], i.e., the researchers use the term 'bridge' to describe what we would today call a wormhole.

This was a brilliant idea, but the mathematical model proposed by the researchers was ill-posed.

The first modern work devoted to this problem was the paper by Wheeler [2] published in 1955. There for the first time a diagram of a wormhole was given. Two years later, Misner and Wheeler, in their well-known paper [3], introduced the term 'wormhole' to the physical community.

Our report is an attempt to prove that some astrophysical objects may be entrances to wormholes. These wormholes seem to be remnants from the inflation phase of the Universe's evolution. The chaotic inflation model is the base of modern cosmology and assumes that there is an infinite number of universes, in addition to ours, which appear in a scalar field in different regions and at different instants of time and form what is known as 'spacetime foam' [4–6]. Primary spacetime tunnels (wormholes) probably exist in the initial scalar field [7] and, possibly, have been retained since inflation [8, 9], connecting different regions of our and other universes (see Fig. 1), which opens the unique possibility of studying the multicomponent Universe and detecting new types of objects — entrances to tunnels.

However, analysis of wormhole models reveals that for wormholes to exist, matter with an unusual equation of state is needed [10–12]. The equation of state must be anisotropic, and $w_{\|} = p_{\|}/\varepsilon$ must be smaller than -1 (as with phantom matter). Here, $p_{\|}$ is the total pressure along the tunnel, and ε is the total energy density of all the components of matter in the tunnel. So far, the existence of such matter has only been an assumption [13]. In what follows, we use the term 'phantom energy' when dealing with an isotropic equation of state, $p/\varepsilon < -1$, and the term 'phantom matter' when we are dealing with an anisotropic equation of state. The units of measurement are selected such that $c = 1$ and $G = 1$.

In our report we consider models in which the main wormhole material with all the necessary properties is a strong magnetic field that penetrates everything, while phantom matter and phantom energy are needed only as a small addition, and models in which the main material is phantom energy with an equation of state close to the vacuum one ($p/\varepsilon = -1$) and the addition of magnetic field energy density. Some observed astronomical objects may turn out to be entrances to tunnels.

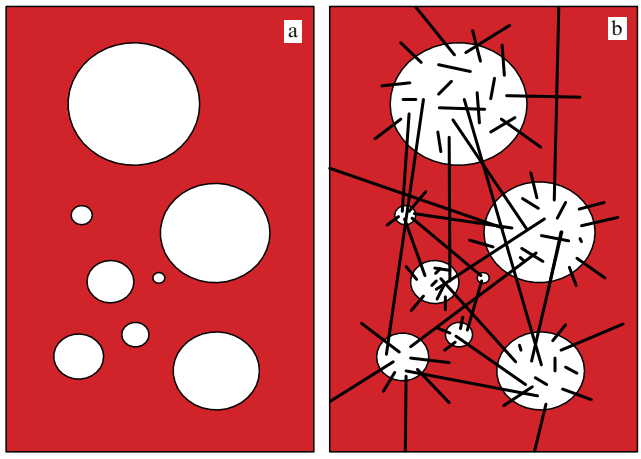

Figure 1. Models of a chaotic inflationary multicomponent Universe (a) without tunnels, and (b) with wormholes.

Uspekhi Fizicheskikh Nauk **177** (9) 1017 – 1028 (2007)
Translated by E Yankovsky; edited by A Radzig

We do not examine the stability of wormholes. Models of wormholes exist for which stability has been proved to exist (see, e.g., paper [14]).

Our hypothesis has been discussed in greater detail in Refs [15–17].

2. A model of a spherically symmetric magnetic wormhole

A static spherically symmetric wormhole is described by the same equations of state as a spherical relativistic star, and the major difference is, by definition, that such a wormhole has a spatial 'neck' creating a multiply connected topology and that there is no horizon.[1] According to Morris and Thorne [18], the metric can be written out as follows:

$$\mathrm{d}s^2 = \exp\bigl(2\phi(r)\bigr)\,\mathrm{d}t^2 - \frac{\mathrm{d}r^2}{1-b(r)/r} - r^2\,\mathrm{d}\Omega^2\,, \tag{1}$$

where r is the radial coordinate, $\phi(r)$ is what is known as the redshift function, and $b(r)$ is the shape function. The wormhole neck corresponds to the minimum $r = r_0 = b(r_0)$ and $b'(r_0) \leqslant 1$. The fact that an object has a horizon is expressed by the condition $\phi \to -\infty$ or $\exp\phi \to 0$, so for a wormhole the function ϕ must be finite. For the spherically symmetric case, the diagonal terms of the energy–momentum tensor are given by [18]

$$\begin{aligned} 8\pi\varepsilon(r) &= \frac{\mathrm{d}b}{\mathrm{d}r}\,\frac{1}{r^2}\,, \qquad 8\pi p_{\parallel}(r) = -\frac{b}{r^3} + 2\left(1-\frac{b}{r}\right)\frac{\mathrm{d}\phi}{\mathrm{d}r}\,\frac{1}{r}\,,\\ 8\pi p_{\perp}(r) &= \left(1-\frac{b}{r}\right)\left[\frac{\mathrm{d}^2\phi}{\mathrm{d}r^2} + \left(\frac{\mathrm{d}\phi}{\mathrm{d}r}\right)^2 + \frac{1}{r}\,\frac{\mathrm{d}\phi}{\mathrm{d}r}\right]\\ &\quad - \frac{1}{2r^2}\left(r\,\frac{\mathrm{d}b}{\mathrm{d}r} - b\right)\left(\frac{\mathrm{d}\phi}{\mathrm{d}r} + \frac{1}{r}\right), \end{aligned} \tag{2}$$

where $\varepsilon(r)$ is the energy density.

We introduce the wormhole mass $M(r)$ for an external observer as follows:

$$M(r) = M_0 + \int_{r_0}^{r} 4\pi\varepsilon r^2\,\mathrm{d}r\,, \tag{3}$$

with $M_0 = r_0/2$.

To make numerical calculations more convenient, we introduce the variable $x = r_0/r$, with the result that the interval $r_0 \leqslant r < \infty$ is transformed into $0 < x \leqslant 1$, and instead of Eqns (2) we have

$$\begin{aligned} 8\pi\varepsilon r_0^2 &= -\frac{b'x^4}{r_0}\,,\\ 8\pi p_{\parallel} r_0^2 &= -\frac{bx^3}{r_0} - 2x^3\left(1-\frac{bx}{r_0}\right)\phi'\,,\\ 8\pi p_{\perp} r_0^2 &= \left(1-\frac{bx}{r_0}\right)\left[x^4\phi'' + x^3\phi' + x^4(\phi')^2\right]\\ &\quad + \frac{0.5x^3(xb'+b)(1-x\phi')}{r_0}\,. \end{aligned} \tag{4}$$

Here, a prime indicates a derivative with respect to x. In Ref. [19], it was shown that in a spherically symmetric wormhole with $w_{\parallel} = \text{const}$ and $w_{\perp} = \text{const}$ the following inequalities determining the possible equations of state and their anisotropy must hold:

$$-2w_{\perp} < w_{\parallel} < -1\,. \tag{5}$$

The left inequality in Eqn (5) specifies the finiteness of the wormhole mass as $r \to \infty$, while the right inequality indicates the absence of a horizon.

It is highly interesting that for a magnetic (or electric) field the conditions specified by (5) are 'almost' met. If the direction of the field coincides with r, the energy–momentum tensor defines the equation of state:

$$w_{\parallel} = -1\,, \quad w_{\perp} = 1\,, \quad \varepsilon = \frac{H^2+E^2}{8\pi}\,, \tag{6}$$

which to within a small negative addition to $w_{\parallel}$ satisfies conditions (5) for a wormhole.

In Ref. [20], a model of a wormhole consisting of phantom matter with an anisotropic equation of state, namely

$$1 + \delta = -\frac{p_{\parallel}}{\varepsilon} = \frac{p_{\perp}}{\varepsilon}\,, \tag{7}$$

was examined, and it was found that for a wormhole to exist it is sufficient that the parameter δ be as small as desired.

We introduce the following notation: $x_{\mathrm{h}} = r_0/r_{\mathrm{h}} > 1$, the ratio of the wormhole neck radius to the radius of the horizon of the respective Reissner–Nordström black hole [21] with a magnetic charge $Q = r_{\mathrm{h}}$. The value of ε is determined by the relationships

$$\varepsilon = \varepsilon_0\,x^4\left(\frac{x_{\mathrm{h}}-1}{x_{\mathrm{h}}-x}\right)^{\delta}, \qquad \varepsilon_0 = \frac{1}{8\pi r_0^2(1+\delta)}\,. \tag{8}$$

The wormhole mass M_{∞} for an observer located far from the neck falls within the interval

$$M_0 \leqslant M_{\infty} \leqslant 2M_0\,. \tag{9}$$

The left inequality in Eqn (9) follows from definition (3), and the right inequality follows from formulas (8).

In this regard, it is possible to conclude that an electromagnetic field may make up a substantial or even the major part of wormhole matter.

The parameters of the neck of a magnetic wormhole with different masses M_0 are listed in Table 1. From Eqn (8) we can derive expressions (with allowance for the constants c and G) for r_0, H_0, the mass density ρ_0, the frequency ν_G of radial vibrations with a minimum amplitude, the gyrofrequency ν_{H} in the neck in its rest frame, and the frequency ν_{c} (for an external observer) of revolution along the lower stable circular orbit:

$$\begin{aligned} r_0 &= \frac{G}{c^2}\,2M_0\,,\\ H_0 &= \frac{c^4}{G^{3/2}}\,(2M_0)^{-1}\,,\\ \rho_0 &= \frac{c^6}{8\pi G^3}\,(2M_0)^{-2}\,,\\ \nu_G &= \frac{c^3}{2\sqrt{2}\,\pi G}\,(2M_0)^{-1}\,,\\ \nu_{\mathrm{H}} &= \frac{ec^3}{2\pi m_{\mathrm{e}} G^{3/2}}\,(2M_0)^{-1}\,,\\ \nu_{\mathrm{c}} &= \frac{\sqrt{3}\,c^3}{32\pi G}\,(2M_0)^{-1} = \sqrt{\frac{3}{128}}\,\nu_G\,. \end{aligned} \tag{10}$$

[1] Here and in what follows we mean an observer's horizon.

Table 1. Parameters of the neck of a magnetic wormhole with different masses.

$M_\infty = 2M_0$	r_0, cm	H_0, G	$\rho(r_0)$, g cm^{-3}	ν_G, Hz	ν_H, Hz	ν_c, Hz
6×10^{42} g $= 3 \times 10^9 M_\odot$ (quasar)	4.5×10^{14}	7.8×10^9	2.7×10^{-3}	7.6×10^{-6} (1.5 days)	2.2×10^{16}	1.16×10^{-6} (9.8 days)
10^{39} g $= 5 \times 10^5 M_\odot$ ($e^\pm$ pair production)	7.4×10^{10}	4.4×10^{13}	9.7×10^4	0.045 (22 s)	1.3×10^{20}	6.9×10^{-3} (2.4 min)
2×10^{33} g $= M_\odot$ (Sun)	1.5×10^5	2.3×10^{19}	2.4×10^{16}	2.3×10^4	6.6×10^{25}	3.5×10^3
6×10^{27} g $= M_\oplus$ (Earth)	0.45	7.8×10^{24}	2.7×10^{27}	7.6×10^9	2.2×10^{31}	1.16×10^9
5×10^{10} g (positronium)	3.5×10^{-18}	10^{42}	4.4×10^{61}	9.7×10^{26}	2.7×10^{48}	1.5×10^{26}
1.8×10^3 g ($\mu^\pm$ pair production)	1.3 × 10−25	2.6×10^{49}	3×10^{76}	2.6×10^{34}	7.3×10^{55}	4×10^{33}
2×10^{-5} g (Planck mass)	1.5×10^{-33}	2.3×10^{57}	2.4×10^{92}	2.3×10^{42}	6.6×10^{63}	3.5×10^{41}

The wormhole parameters in Table 1 have been estimated for a quasar nucleus, objects with a critical field (and respective wormhole mass) needed for electron–positron pair production, objects whose mass is on order of the Sun's and Earth's masses, objects with a critical magnetic field (and respective wormhole mass) in which a positronium atom is stable, objects with a critical magnetic field (and mass) needed for monopole–antimonopole pair production, and objects with Planck mass.

Expression (1) for the metric was deduced with respect to Schwarzschild's coordinate system. The physical coordinate l measuring the distance along the tunnel encompasses both entrances $(-\infty < l < +\infty)$ and is related to the radial coordinate r by the following formula

$$l(r) = \pm \int_{r_0}^{r} \frac{\mathrm{d}r}{\sqrt{1 - b_\pm(r)/r}} \,. \tag{11}$$

For $r \gg r_0$, we have $l \to r$, and for a model described by formulas (8) with a small δ, the magnetic field strength equals

$$H \approx \frac{2M_0\sqrt{G}}{r^2} \,. \tag{12}$$

If we assume that the electric field is weak, the restriction related to electron–positron pair production is lifted, but Table 1 lists only the limiting intensity of the field, $H_{\mathrm{lim}} = m_e^2 c^3/(\mu\hbar) \approx 4.4 \times 10^{13}$ G, corresponding to this restriction. This field strength determines the specific conditions related to the fact that for $H > H_{\mathrm{lim}}$ the Landau excitation level exceeds the electron rest energy. In a field stronger than 10^{42} G, the positronium atom becomes stable and the medium gets filled by these atoms produced from vacuum [22, 23]. In magnetic fields stronger than the critical field H_{max}, the vacuum breaks down and monopole pairs are produced [24–26]. If the mass m_μ of a stable colorless monopole of the 't Hooft–Polyakov type [27–29] is of order 10^{16} GeV $\sim 10^{-8}$ g, the magnetic charge $\mu = (3/2)\hbar c/e \sim 10^{-7}$, and $H_{\mathrm{max}} = m_\mu^2 c^3/(\mu\hbar) \approx 2.6 \times 10^{49}$ G, then the maximum mass of a magnetic wormhole with such a field in the neck is, according to formulas (10), $2M_0 \approx 1.8$ kg. The monopoles being produced will leave the wormhole, thus reducing its mass. In relation to other quantum processes, the stability of such small wormholes is not obvious, with the result that the minimum wormhole mass may prove to be much larger than 1.8 kg. The lower limit for the mass of composite wormholes is, obviously, even smaller. We also note that the absence of a horizon for wormholes means that they do not evaporate (the Hawking effect). Hence, primary wormholes with a small mass could have survived up to this day, in contrast to primordial black holes whose lower bound on mass is about 10^{15} g.

3. Entrances into tunnels and black holes with a magnetic field in the Galaxy and in galactic nuclei

The model considered is Section 2 presupposes that among galactic and extragalactic objects one can detect entrances into tunnels or black holes formed as a result of evolution from primordial wormholes. From the above discussion it also appears that these black holes may differ from primordial black holes in the magnitude and structure of the magnetic field.

The presence of a radial magnetic field can be detected from the specific law of the field intensity variation ($H \propto r^{-2}$) and the same sign of the magnetic field on all sides. The rotation of a monopole generates a dipole electric field which can accelerate the relativistic particles. What is important is that a dipole electric field (in contrast to the quadrupole field for a disk) accelerates electrons in the direction of one pole, while protons and positrons are accelerated in the direction of the other pole. This allows an explanation within the framework of the model in question of the origin of unidirectional jets from some sources (e.g., the quasar 3C273) [30].

The presence of an accretion disk complicates the picture. A quadrupole electric field generates bidirectional jets of electrons or protons/positrons (depending on the sign of the quadrupole). As a result, we may be faced with different jet structures. The interaction effects of the electromagnetic fields of a wormhole/black hole and the accretion disk are probably very strong.

The difference between the entrance to a wormhole and a black hole can be detected by the absence of a horizon: a luminous source falling into a wormhole will be observed continuously but with variable redshift or even blue shift. Here, however, we must assume that the tunnel is transparent.

A blue shift may emerge if the mass of the opposite entrance (in relation to the observer) to the wormhole is

larger than the mass of the closest entrance. If the tunnel is transparent and there are accretion disks at both entrances, the redshifts for the spectra of these disks will also be different: two different redshifts of a single source related to the wormhole could be detected.

The observed image of a wormhole may exhibit an inner structure with angular dimensions much smaller than those determined by the gravitational diameter.

In this respect, the observed data on the gravitational lensing of the quasar Q0957+561 with a redshift $z = 1.4141$ [31] is very interesting, since it follows that the sizes of this quasar are much smaller than the Schwarzschild diameter. A specific feature of a wormhole that demonstrates strong relativistic effects and at the same time the absence of a horizon is the possibility of periodic vibrations of a test mass in relation to the neck (see Table 1 and Appendix 1). Here, the redshift of this mass also varies periodically. If the structure of the wormhole is close to horizon formation, the values of these shifts, their period, and the flux oscillations may be very large. In view of this one should mention the observations of quasiperiodic variations in the flux of such objects as IDV-sources (IDV stands for Intra Day Variability), say from the Lacerta object 0716+714 [32].

When sources move along circular orbits about the entrance to a tunnel (see Table 1 and Appendix 2), a compact source will also have a variable flux and redshift. Finally, an external observer can detect radiation at gyrofrequencies and phenomena related to $e^{\pm}$- and $\mu^{\pm}$-pair production.

4. Conclusions and prospects

We believe that the main conclusion that can be drawn from the above discussion is the possibility of detecting among known galactic and extragalactic objects usually identified as black holes with stellar masses and masses on the order of galactic nuclei new types of primary cosmological objects — entrances into wormholes or specific black holes that have formed from wormholes. The conclusion is also important here that there is a strong magnetic field with a radial structure (the Hedgehog model [33, 34]), which ensures, with allowance for rotation, the generation of jets of relativistic particles (unidirectional or bidirectional outbursts). For such objects, the wormhole models assume the presence of specific effects associated with the absence of a horizon and ensuring that the sources of radiation are visible at any point of the tunnel, provided that the medium is transparent. What they also assume is that the variations of the spectrum, flux, and polarization of the luminous source follow a definite law. New effects of gravitational lensing on wormholes are expected to be detected (see Refs [20, 35]). Also, it is possible that quasiperiodic vibrations of luminous objects in relation to the wormhole neck will be discovered.

It is possible to study the structure of candidates, i.e., sources related to the entrances to wormholes (or black holes) with a radial magnetic field, with instruments whose angular resolution amounts to several milliseconds of arc and even better; such a study is scheduled for conducting with the space interferometers in the RadioAstron [36] and Millimetron [37] projects.

It seems possible that the radiation sources will be discovered that are associated with double entrances into tunnels; these entrances form systems with strong magnetic dipole radiation and ejection of relativistic $e^{\pm}$. The final stage of evolution of such systems would conclude with creating the black hole and generating the high-power electromagnetic pulses.

It is also important to emphasize that the presence of wormholes with strong magnetic fields makes it possible to assume that the elementary magnetic monopoles predicted in Refs [33, 34] may have been absorbed by these objects in the process of cosmological evolution.

Another area of research is related to the spectral and polarization monitoring of the radiation from these sources.

The discovery of tunnels opens the path to possible studies of the entire multicomponent Universe.

Appendices

Appendix 1. The observation of a body vibrating with respect to the neck of a wormhole

A specific phenomenon may be the vibrations of bodies near the neck of a wormhole (radial orbits). Signals from such sources, reaching an external observer, exhibit a characteristic periodicity in their spectrum. All other objects except wormholes (stars and black holes) irrevocably absorb the radiation falling on them. Periodic radial vibrations constitute a specific feature of wormholes.

To simplify matters, let us take a test body with zero angular momentum. To solve the equations of motion we use the Hamilton – Jacobi method in curved space [38].

For the body's velocity we then have

$$\frac{\partial r}{\partial t} = \pm \exp\phi \sqrt{\left(1 - \frac{b}{r}\right)\left[1 - \exp(2\phi)\left(\frac{m_0}{E_0}\right)^2\right]}, \qquad (13)$$

where m_0 and E_0 are the rest mass and total energy of the body, respectively. Since, for a wormhole, $\exp\phi > 0$ in the entire space, the equation $\dot{r} = 0$ has three roots: two of them correspond to the second factor in the square brackets of the integrand in Eqn (13) being zero (stopping of the body on two sides of the neck), and the third corresponds to the first factor in the integrand being zero (stopping at the neck).

Let us discuss the stopping at the neck more thoroughly. This is a unique phenomenon related solely to the curvature of space. First, we verify that this stopping takes a finite time. For this we examine the integral

$$\Delta t = \int_{r_0}^{r_1} \frac{\mathrm{d}r}{\dot{r}}\,. \qquad (14)$$

The integral is not divergent if the r-derivative of $1 - b/r$ is nonzero in the neck. That this is the case follows from the expression for the wormhole metric. From the fact that integral (14) is finite follows the finiteness of the time it takes the body to stop in the neck (and, for similar reasons, the entire cycle of vibrations is also finite).

Expression (13) does not give the physical velocity of the body, since the coordinate r is not the physical radial coordinate — it is l that represents such a coordinate in Eqn (11). According to this, we find the physical velocity $\dot{l}$ of the body along the radius:

$$\dot{l} = \pm \exp\phi \sqrt{1 - \exp(2\phi)\left(\frac{m_0}{E_0}\right)^2}\,. \qquad (15)$$

This velocity no longer vanishes at the wormhole neck.

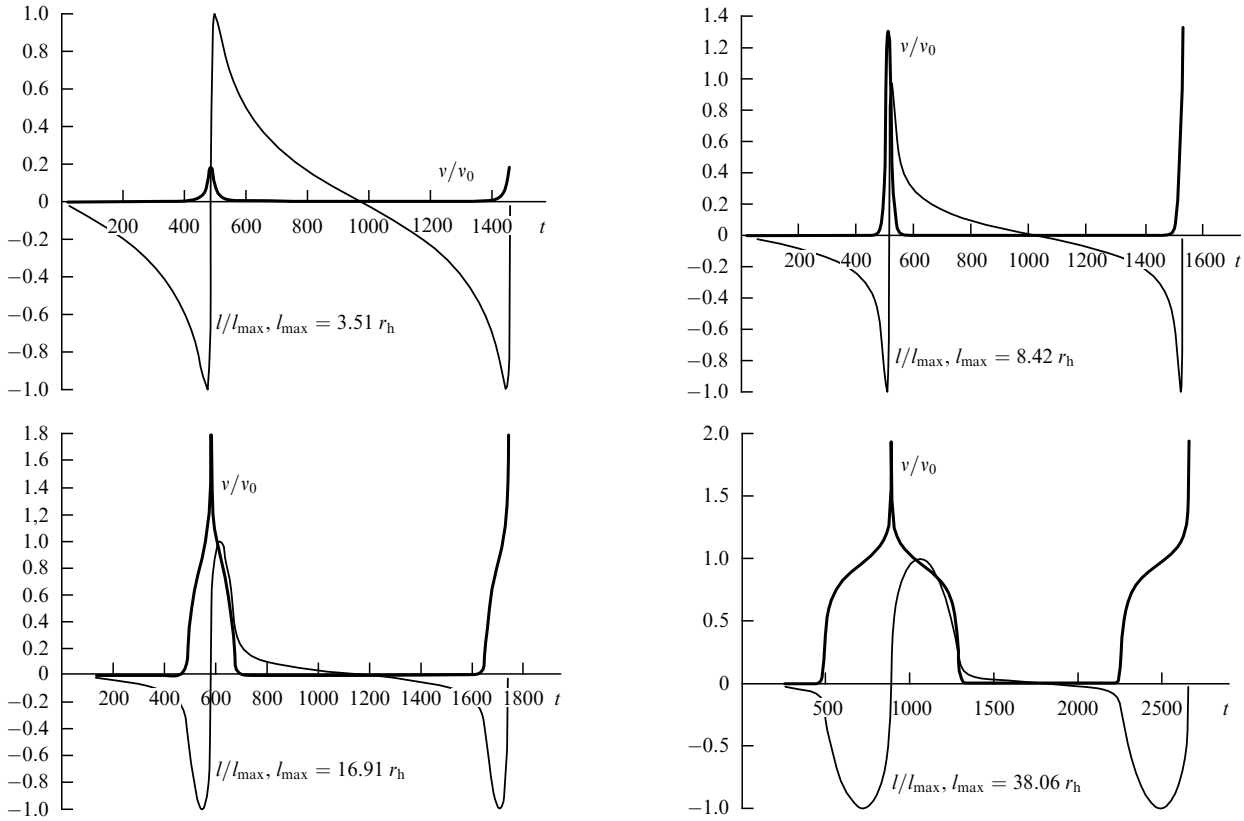

Figure 2. Dependences of the frequency shift v/v_0 (heavy curves) and of the shift in the physical radial coordinate $l/l_{\max}$ (light curves) on time t (in units of r_h/c). The diagrams are constructed for $\delta = 0.001$.

The redshift of the signal emitted by the body is determined by two factors:

(i) the Doppler shift from the motion of the source: the factor $\sqrt{1-v^2}/(1 \pm v)$, where $v = \dot{r}\sqrt{|g_{rr}/g_{tt}|}$ is the physical velocity of the body in its proper time (here the plus sign corresponds to the body's motion away from the observer, and the minus sign toward the observer, and g_{rr} and g_{tt} are the components of the metric tensor);

(ii) the gravitational redshift: the factor $\exp\phi$.

Hence, the frequency of the signal for a distant observer will be determined by the expression

$$v = v_0 \frac{\exp(2\phi)(m_0/E_0)}{1 \pm \sqrt{1-\exp(2\phi)(m_0/E_0)^2}}\,, \tag{16}$$

where v_0 is the frequency of the signal measured on the moving body. This shows that at the wormhole neck, in contrast to the black hole horizon, the frequency of the signal does not go to zero for a distant observer.

In order to find, for an external observer, the time dependence of the redshift v/v_0 of the body, we must add to t the time Δt it takes light to travel from point r to point $r_{\max}$ of the body. The corresponding diagrams are shown in Fig. 2.

For extremely small amplitudes $r_1 - r_0$, the vibrations of the test body become harmonic. This is achieved if the following inequalities hold:

$$r - r_0 \leqslant r_1 - r_0 \ll r_0 - r_h\,, \quad 1 - x \leqslant 1 - x_1 \ll x_h - 1\,, \tag{17}$$

where $x_1 = r_0/r_1$. In this case, near the stopping points of the body the components of its velocity $\dot{r}$ (13) can be represented by series expansions in powers of $1 - x$ (or in powers of $x - x_1$). Leaving only the leading terms, we find that

$$\exp\phi \approx x_h - 1\,, \quad 1 - \frac{b}{r} \approx (x_h - 1)(1 - x)\,,$$
$$1 - \exp(2\phi)\left(\frac{m_0}{E_0}\right)^2 \approx \frac{2(x - x_1)}{x_h - 1}\,. \tag{18}$$

This leads us to the equation of motion for a harmonic oscillator with stopping points at $x = 1$ and $x = x_1$:

$$(\dot{r})^2 \approx 2(x_h - 1)^2(1 - x)(x - x_1)\,,$$
$$r_h\ddot{r} = \dot{r}\frac{\partial\dot{r}}{\partial x} = \frac{1}{2}\frac{\partial(\dot{r})^2}{\partial x}\,, \tag{19}$$
$$(1 - x)^{\cdot\cdot} = -\omega_0^2(1 - x)\,,$$

where $\omega_0 = \sqrt{2}\,(x_h - 1)/r_h$. To an external observer, the period of such oscillations appears as

$$T_1 = \frac{\sqrt{2}\,\pi r_h}{c(x_h - 1)}\,. \tag{20}$$

Here, the oscillations of the physical coordinate l are also harmonic, which follows from Eqns (11), (15), and (18). The body oscillates from $-l_1$ to $+l_1$, and the condition of smallness for l_1, corresponding to Eqn (17), is given by the inequality $l_1 \ll r_h$ (thus, in terms of these coordinates the amplitude is not necessarily extremely small).

The oscillations of the coordinate l have twice as big a period ($T_2 = 2T_1$), since the physical velocity $\dot{l}$ has two stopping points (rather than three, as $\dot{r}$ has). This can easily be verified by calculating the period directly from Eqn (14).

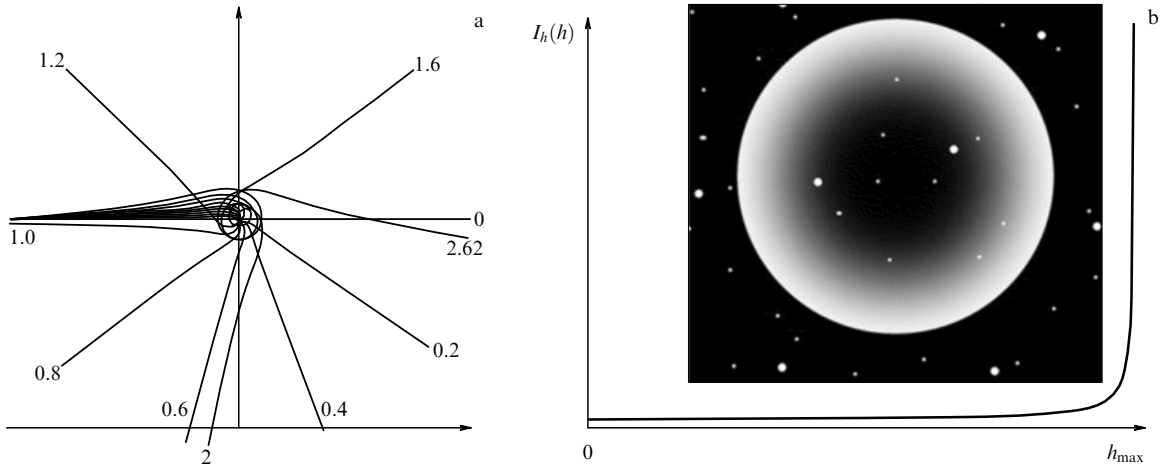

Figure 3. (a) Deflection of photons traveling through the neck of a wormhole (the number alongside each curve specifies the value of the impact parameter). (b) Dependence of the intensity I_h of light traveling through the neck of a wormhole on the impact parameter h.

Appendix 2. Circular orbits of a test particle about a wormhole

Let us find the limiting circular orbits of a test particle about a wormhole. For this we first solve this problem in the metric of the limiting Reissner – Nordström spacetime [with the Hamilton – Jacobi method (see Ref. [38])].

For the specific angular momentum of the particle we introduce the notation $\lambda = L/(m_0 r_\mathrm{h} c)$.

In accordance with Refs [39, 40], the specific effective potential energy $U(x)$ of the test particle and its derivative take, respectively, the form

$$U(x) = (1-x)\sqrt{1+\lambda^2 x^2}\,, \qquad U'(x) = -\frac{2\lambda^2 x^2 - \lambda^2 x + 1}{\sqrt{1+\lambda^2 x^2}}\,. \tag{21}$$

The roots for the unstable and stable circular orbits can be found from the condition $U'(x) = 0$:

$$x_\pm = 0.25\left(1 \pm \sqrt{1-\frac{8}{\lambda^2}}\right). \tag{22}$$

Hence follows that $\lambda^2 \geqslant 8$.

Therefore, the last stable orbit corresponds to

$$x_- = \frac{1}{4}\,, \qquad r_- = 4r_\mathrm{h}\,, \qquad \lambda^2 = 8\,, \tag{23}$$

while the last unstable circular orbit corresponds to

$$x_+ = \frac{1}{2}\,, \qquad r_+ = 2r_\mathrm{h}\,, \qquad \lambda^2 \to \infty\,. \tag{24}$$

The same method can be used to derive an expression for $\dot\varphi = \mathrm{const}$ on a circular orbit, and an expression for the revolution period

$$\tau = \int_0^{2\pi} \frac{\mathrm{d}\varphi}{\dot\varphi} = \frac{2\pi r^2 E_0/L}{c^2(1-r_\mathrm{h}/r)^2}\,, \tag{25}$$

where $E_0 = U(r)$ for the specific circular orbit.

From this we can find the periods (measured by a clock of a distant observer) of the last stable and unstable circular orbits:

$$\tau(4r_\mathrm{h}) = \frac{32\pi r_\mathrm{h}}{\sqrt{3}c}\,, \qquad \tau(2r_\mathrm{h}) = \frac{8\pi r_\mathrm{h}}{c}\,. \tag{26}$$

When $r \geqslant 2r_\mathrm{h}$, for a wormhole we can ignore the corrections related to δ. Hence, results (23) – (26) would also hold for wormholes.

Appendix 3. The characteristic distribution of the intensity of light passing through a wormhole

The angles of the deflection of photons traveling through the neck of a wormhole with the parameters $w_\perp = -w_\parallel = 2$ have been calculated in Ref. [19] (Fig. 3a). Using this result, one can construct the angular dependence of the intensity of light traveling through the wormhole's neck (see Ref. [20]).

We examine the case of a uniform (on the average) distribution of light sources from the side of a wormhole opposite an observer (e.g., the cosmological background). Then, in the spherically symmetric version, the wormhole neck on the average is illuminated uniformly from all sides.

We analyze the light that travels through the wormhole neck in the equatorial plane (i.e., in the plane $\theta = \pi/2$). On the observer's side, the intensity of the light passing through the neck will depend on the impact parameter h (measured in units of the neck radius r_0).

Let φ be the angle of deflection of a photon after it has passed through the neck (as a result of gravitational lensing), and I_tot be the total intensity of light from different directions of angle φ, with $I_\varphi \equiv \mathrm{d}I_\mathrm{tot}/\mathrm{d}\varphi$ being the intensity density per unit angle. We have $I_\varphi = \mathrm{const}$ (in view of the fact that the intensity does not depend on the direction of light propagation beyond the neck).

Then, one obtains

$$\frac{\mathrm{d}I_\mathrm{tot}}{\mathrm{d}h} \equiv I_h(h) = \frac{\mathrm{d}I_\mathrm{tot}}{\mathrm{d}\varphi}\frac{\mathrm{d}\varphi}{\mathrm{d}h} = \mathrm{const}\,\frac{\mathrm{d}\varphi}{\mathrm{d}h}\,.$$

The function $\varphi(h)$ was found in Ref. [19]:

$$\varphi(h) = 2\int_1^\infty \frac{h}{x^2\sqrt{(1-y/x)\left(\exp(-2\phi) - h^2/x^2\right)}}\,\mathrm{d}x\,. \tag{27}$$

Introducing the notation $1/x \equiv q$, we get

$$I_h(h) = C \int_0^{q_0} \frac{\exp(-2\phi)\,\mathrm{d}q}{\sqrt{1-qy}\left[\exp(-2\phi) - q^2h^2\right]^{3/2}}\,. \qquad (28)$$

This intensity distribution in h is minimal at the zero impact parameter and maximal at maximum impact parameters corresponding to the width of the wormhole neck, with this result being independent of the wavelength of the light traveling through the wormhole.

A characteristic diagram for $I_h(h)$ is shown in Fig. 3b. It corresponds to a wormhole with metric (1). Thus, the observer will see a ring of light with sharp outer edges and smeared inner edges.

With sufficiently high resolution of the observational devices, this fact can make it possible to distinguish between wormholes and black holes in, say, active galactic nuclei.

References

1. Einstein A, Rosen N *Phys. Rev.* **48** 73 (1935)
2. Wheeler J A *Phys. Rev.* **97** 511 (1955)
3. Misner C W, Wheeler J A *Ann. Phys.* (New York) **2** 525 (1957)
4. Wheeler J A *Ann. Phys.* (New York) **2** 604 (1957)
5. Vilenkin A *Phys. Rev. D* **27** 2848 (1983)
6. Linde A D *Phys. Lett. B* **175** 395 (1986)
7. Visser M *Lorentzian Wormholes: from Einstein to Hawking* (Woodbury, NY: AIP, 1995)
8. Lobo F S N *Phys. Rev. D* **71** 084011 (2005)
9. Shinkai H, Hayward S A *Phys. Rev. D* **66** 044005 (2002)
10. Rahaman F et al. *Phys. Lett. B* **633** 161 (2006); gr-qc/0512075
11. Kuhfittig P K F *Phys. Rev. D* **73** 084014 (2006); gr-qc/0512027; Lobo F S N *Phys. Rev. D* **71** 124022 (2005); gr-qc/0506001
12. Visser M, Kar S, Dadhich N *Phys. Rev. Lett.* **90** 201102 (2003); gr-qc/0301003
13. Jassal H K, Bagla J S, Padmanabhan T *Phys. Rev. D* **72** 103503 (2005)
14. Armendáriz-Picón C *Phys. Rev. D* **65** 104010 (2002); gr-qc/0201027
15. Kardashev N S, Novikov I D, Shatskii A A *Astron. Zh.* **83** 675 (2006) [*Astron. Rep.* **50** 601 (2006)]
16. Kardashev N S, Novikov I D, Shatskiy A A *Int. J. Mod. Phys. D* **16** 909 (2007)
17. Kardashev N S, Novikov I D, Shatskiy A A, astro-ph/0610441
18. Morris M S, Thorne K S *Am. J. Phys.* **56** 395 (1988)
19. Shatskii A A *Astron. Zh.* **81** 579 (2004) [*Astron. Rep.* **48** 525 (2004)]
20. Shatskii A A *Astron. Zh.* **84** (2) 99 (2007) [*Astron. Rep.* **51** 81 (2007)]
21. Misner C W, Thorne K S, Wheeler J A *Gravitation* (San Francisco: W.H. Freeman, 1973) [Translated into Russian: Vol. 3 (Moscow: Ainshtain, 1997)]
22. Shabad A E, Usov V V, hep-th/0512236
23. Shabad A E, Usov V V, in *Particle Physics at the Year of 250th Anniversary of Moscow University: Proc. of the 12th Lomonosov Conf. on Elementary Particle Physics, Moscow, Russia, 25–31 August 2005* (Ed. A I Studenikin) (Singapore: World Scientific, 2006); astro-ph/0601542
24. Bander M, Rubinstein H R *Phys. Lett. B* **280** 121 (1992)
25. Duncan R C, astro-ph/0002442
26. Peng Q, Chou C *Astrophys. J.* **551** L23 (2001)
27. 't Hooft G *Nucl. Phys. B* **79** 276 (1974)
28. Polyakov A M *Pis'ma Zh. Eksp. Teor. Fiz.* **20** 430 (1974) [*JETP Lett.* **20** 194 (1974)]
29. Kibble T W B *J. Phys. A: Math. Gen.* **9** 1387 (1976)
30. Stawarz L *Astrophys. J.* **613** 119 (2004)
31. Schild R E, Leiter D J, Robertson S L, astro-ph/0505518
32. Ostorero L et al., astro-ph/0602237
33. Kardashev N S "Posleslovie k russkomu izdaniyu" ("Afterward to the Russian edition"), in: Burbidge G, Burbidge M *Kvazary* (Quasi-Stellar Objects) (Moscow: Mir, 1969)
34. Kovalev Yu A, Kovalev Yu Yu, Nizhelsky N A *Publ. Astron. Soc. Jpn.* **52** 1027 (2000)
35. Cherepashchuk A M *Vestn. Mosk. Univ. Fiz. Astron.* **60** (2) 62 (2005) [*Moscow Univ. Phys. Bull.* **60** (2) 74 (2005)]
36. RadioAstron Mission, http://www.asc.rssi.ru/radioastron/description/intro_eng.htm
37. Millimetron Project, http://www.asc.rssi.ru/millimetron/eng/millim_eng.htm
38. Landau L D, Lifshitz E M *Teoriya Polya* (The Classical Theory of Fields) (Moscow: Nauka, 1995) [Translated into English (Boston: Butterworth–Heinemann, 1987)]
39. Frolov V P, Novikov I D *Black Hole Physics: Basic Concepts and New Developments* (Dordrecht: Kluwer, 1998)
40. Carr B J "Primordial black holes: do they exist and are they useful?", astro-ph/0511743

PACS numbers: **95.35+d**, **98.80.–k**
DOI: 10.1070/PU2007v050n09ABEH006382

Dark matter: from initial conditions to structure formation in the Universe

V N Lukash, E V Mikheeva

1. "Bring me that, don't know what"

We are at the verge of a discovery capable of changing the essence of our world view. We are talking about the nature of dark matter.

Recently, astronomy has taken important steps in observational justification for dark matter, and today the presence of dark matter in the Universe can be considered a firmly established fact. What makes the situation so special is that astronomers *observe* structures made of matter *unknown* to physicists. This has posed the problem of identifying the physical nature of such matter.

Modern elementary particle physics knows of no particles that have the properties of dark matter. This requires an extension of the Standard Model. But how and in what direction should we move, and what and where should we look for? The heading of this section, a quotation from a Russian fairy tale, very fittingly reflects the current situation.

Physicists are looking for the unknown particles, having only a general idea about the properties of the observed matter. But what are these properties?

The only thing we know for certain is that dark matter interacts with a luminous matter (baryons) in the gravitational way and constitutes a cold medium with a cosmological density several times higher than the baryon density. In view of such simple properties, dark matter directly affects the development of the gravitational potential of the Universe. The contrast of its density grew with time, leading to the formation of gravitationally bound systems of dark-matter halos.

It should be emphasized that this process of development of gravitational instability could be triggered in the Friedmann Universe only in the presence of primordial density perturbations, whose very existence is in no way related to dark matter but instead is caused by Big Bang physics. Hence, we face another important question of how these seed perturbations, from which the structure of dark matter developed, emerged.

We will turn our attention to the problem of generation of primordial cosmological perturbations somewhat later. Let us now return to dark matter.

Baryons are trapped by the gravitational wells of dark matter concentrations. Hence, although the particles of dark

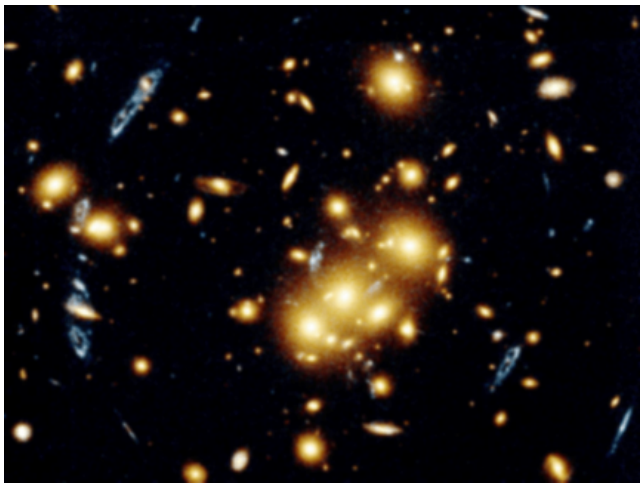

Figure 1. A region of the sky in the direction of the 0024+1654 cluster of galaxies. The picture was taken by the Hubble Space Telescope.

matter do not interact with light, there is light where there is dark matter. This remarkable property of gravitational instability has made it possible to study the amount, state, and distribution of dark matter from observational data from the radio range to the X-ray range.

An independent corroboration of our conclusions concerning the properties of dark matter and other parameters of the Universe is presented by data on the anisotropy and polarization of the cosmic microwave background (CMB), the abundance of light elements in the Universe, and the distribution of absorption lines in the spectra of distant quasars. Numerical simulations, which replaced experiments in cosmological studies, are now being widely used. Valuable information on the distribution of dark matter is contained in numerous observational data on the gravitational lensing of distant sources by nearby clusters of matter.

Figure 1 displays a region of the sky in the direction of one such cluster of dark mass ($\sim 10^{14} M_{\odot}$). We see a cluster of galaxies trapped by the gravitational field of this cluster, hot X-ray gas residing at the bottom of the gravitational potential well, and a multiple image of one of the galaxies of the background that happened to be in the line of sight of the dark halo.

Table 1 lists the average values of various cosmological parameters obtained from astronomical observations (with 10% accuracy). Obviously, the total energy density of all types of particles in the Universe is not higher than 30% of the total critical density (the neutrino contribution does not exceed a few percent). The other 70% 'belongs' to an entity that takes no part in the gravitational 'clustering' of matter. Only the cosmological constant or its generalization, i.e., the medium with negative pressure $\left(|\varepsilon + p| \ll \varepsilon\right)$ that became known as 'dark energy', exhibit such a property. Determining the nature of this dark energy is a goal in the future development of physics.

Table 1. The main cosmological parameters.

Hubble's constant	$h = 0.7$
CMB temperature	$T = 2.725$ K
Curvature of space	$\Omega_{\varkappa} = 0$
Cosmological density of baryons	$\Omega_{\mathrm{B}} = 0.05$
Cosmological density of dark matter	$\Omega_{\mathrm{DM}} = 0.23$
Cosmological density of dark energy	$\Omega_{\Lambda} = 0.7$
Tilt of density perturbations spectrum	$n_S = 0.96$

The present report is devoted to problems of physical cosmology that can be expected to be solved in the nearest future. The primary problem is to determine the initial conditions needed for the formation of dark-matter structures and the search for unknown particles themselves.

2. Early Universe and late Universe

The observed structure of the Universe is the result of the combined action of the initial conditions and the evolution of the density perturbations field. Modern observational data have allowed scientists to determine the characteristics of the density perturbations field in different epochs of its development. This has made it possible to separate information about the initial conditions and the conditions of evolution. Thus, independent studies on the physics of the early and the late Universe have been initiated.

In modern cosmology, the early Universe is understood as a stage of accelerated expansion with the subsequent transition to the hot phase of evolution. We do not know parameters of the Big Bang. There are only the upper bounds [see Eqn (12) in Section 3]. However, there exists a well-developed theory of the generation of cosmological perturbations, where we can calculate spectra of initial density perturbations of matter and primary gravitational waves as functions of the cosmological parameters.

The reasons why commonly accepted model of the early Universe is absent, stem from stability of the predictions of the inflationary Big Bang paradigm — the facts that the generated spectra are close to the flat one, the amplitude of cosmological gravitational waves is relatively small, the geometry of the visible part of the Universe is three-dimensional Euclidean, etc. All these results can be obtained within a broad class of model parameters. The key point in building up a model of the early Universe would be discovery of cosmological gravitational waves. We believe that this can be realized if the space mission *Planck* (starting in 2008) will be successful.

Our knowledge about the late Universe is drastically different. We have here rather precise model, we know the composition of matter, the laws governing the development of the structure, and the values of the cosmological parameters (see Table 1), but at the same time we have no commonly accepted theory describing the origin of the components of matter.

The known properties of the visible part of the Universe make it possible to describe its geometry in terms of the perturbation theory. The amplitude of cosmological perturbations is a small parameter (10^{-5}).

In the zeroth order, the Universe can be described by the Friedmann model specified by a single function of time — the scale factor $a(t)$. The first order is somewhat more complicated. The metric perturbations are the sum of three independent modes: the scalar mode $S(k)$, the vector mode $V(k)$, and the tensor mode $T(k)$, characterized by the spectral functions of the wave number k. The scalar mode describes cosmological density perturbations, the vector mode is responsible for the vortex motion of matter, and the tensor mode is gravitational waves. Thus, the entire geometry is described by four functions: $a(t)$, $S(k)$, $V(k)$, and $T(k)$, of which today we know only the first two (within certain ranges of definition).

The Big Bang represented a catastrophic process of rapid expansion accompanied by an intense, rapidly varying gravitational field. In the course of cosmological expansion, metric perturbations were spontaneously generated in a parametric manner from vacuum fluctuations, as any massless degrees of freedom are generated under the action of an external variable field. Analysis of the observational data favors the quantum-gravitational mechanisms of generation of the primordial perturbations. Thus, the large-scale structure of the Universe is an example of solving the problem of measurability in quantum-field theory.

Here are the main properties of the generated perturbation fields: Gaussian statistics (random distributions in space), a preferential temporal phase (the 'growing' branch of perturbations), the absence of a characteristic scale within a broad range of wavelengths, and a nonzero amplitude of gravitational waves. The last property plays a decisive role in building models of the early Universe, since, coupled most simply to the background metric, gravitational waves carry direct information about the energy scale of the Big Bang.

As the scalar perturbation mode develops, galaxies and other astronomical objects form. An important achievement in recent years [the Wilkinson Microwave Anisotropy Probe (WMAP) experiment] was the impressive refinement of our knowledge concerning the CMB anisotropy and polarization. They emerged long before galaxies were formed as a result of acting all three cosmological perturbation modes on the distribution of relic photons.

Combined analysis of the observational data on the distribution of galaxies and on the CMB anisotropy made it possible to separate the starting conditions and the evolution. Taking into account that the sum $S + V + T \approx 10^{-10}$ is fixed by the value of the CMB anisotropy, one can obtain the upper bound on the vortex and tensor perturbation modes in the Universe (their detection is only possible if the accuracy of observation becomes higher):

$$\frac{V+T}{S} < 0.2\,. \tag{1}$$

If inequality (1) were not true, the amplitude of primordial density perturbations would be insufficient for the formation of the observed structure.

3. In the beginning was sound...

The effect of the quantum-gravitational creation of massless fields has been thoroughly studied. For instance, particles of matter can be produced in this way (e.g., see Refs [1, 2]) (although, in particular, relict photons appeared as a result of the decay of protomatter in the early Universe). The same is true of the generation of gravitational waves [3] and density perturbations [4], since these fields also belong to massless fields and their creation is not forbidden by a threshold energy condition. The problem of how vortex perturbations are generated is still awaiting a solution.

The theory of S and T perturbation modes in a Friedmann Universe is reduced to the quantum-mechanical problem of independent oscillators $q_k(\eta)$ placed in an external parametric field $\alpha(\eta)$ in the Minkowski world with a time coordinate $\eta = \int \mathrm{d}t/a$. The action integral and Lagrangian of these elementary oscillators depend on their spatial frequency $k \in (0, \infty)$:

$$S_k = \int L_k \,\mathrm{d}\eta\,, \qquad L_k = \frac{\alpha^2}{2k^3}(q'^2 - \omega^2 q^2)\,, \tag{2}$$

where the prime indicates a time (η) derivative, $\omega = \beta k$ is the oscillator frequency, and β is the perturbation propagation velocity expressed in units of the speed of light in vacuum (here and in what follows, $c = \hbar = 1$, and the subscript k has been dropped from the field q). In the case of the T mode, $q \equiv q_T$ is the transverse-traceless component of the metric tensor, with

$$\alpha_T^2 = \frac{a^2}{8\pi G}\,, \qquad \beta = 1\,, \tag{3}$$

and in the case of the S mode, $q \equiv q_S$ is a linear superposition of the longitudinal gravitational potential (a perturbation of the scale factor) and the potential of the 3-velocity of the medium multiplied by the Hubble parameter [4], with

$$\alpha_S^2 = \frac{a^2\gamma}{4\pi G\beta^2}\,, \qquad \gamma = -\frac{\dot{H}}{H^2}\,, \qquad H = \frac{\dot{a}}{a}\,, \tag{4}$$

where the over-dot indicates a time (t) derivative.

As formulas (3) suggest, the field q_T is more fundamental than q_S, since it is minimally coupled to the background metric and is independent of the properties of matter (in General Relativity, the velocity of gravitational waves is equal to the speed of light). As for q_S, its coupling to the external field (4) is more complicated: it includes the derivatives of the scale factor and some characteristics of the matter (e.g., the velocity at which perturbations propagate in a medium). We know nothing about protomatter in the early Universe, there are only the general approaches to this problem.

Usually, the medium is assumed to be ideal with its energy–momentum tensor depending on the energy density ε, pressure p, and 4-velocity u^μ of matter. For the S mode, the 4-velocity is potential and can be represented by the gradient of a 4-scalar ϕ:

$$T_{\mu\nu} = (\varepsilon + p)u_\mu u_\nu - p g_{\mu\nu}\,, \qquad u_\mu = \frac{\phi_{,\,\mu}}{w}\,, \tag{5}$$

where $w^2 = \phi_{,\,\mu}\phi_{,\,\nu}\, g^{\mu\nu}$ is a normalization function, with the comma in the subscript indicating a coordinate derivative. The speed of sound appears in the 'equation of state' as a proportionality factor between the comoving perturbations of pressure and energy density of matter:

$$\delta p_\mathrm{c} = \beta^2\, \delta\varepsilon_\mathrm{c}\,, \tag{6}$$

where $\delta X_\mathrm{c} \equiv \delta X - v\dot{X}$, and $v \equiv \delta\phi/w$ is the potential of the 3-velocity of the medium.

In the linear order of the perturbation theory, the concept of an ideal medium is equivalent to the field concept where the Lagrangian density $L = L(w, \phi)$ is assigned to the matter field ϕ. In the field approach, the rate at which perturbations propagate is found from the equation [4–6]

$$\beta^{-2} = \frac{\partial \ln|\partial L/\partial w|}{\partial \ln|w|}\,, \tag{7}$$

which also corresponds to Eqn (6). In most models of the early Universe, it is assumed that $\beta \sim 1$ (in particular, at the radiation-dominated stage $\beta = 1/\sqrt{3}$).

The evolution of elementary oscillators is described by the Klein–Gordon equation

$$\bar{q}'' + (\omega^2 - U)\bar{q} = 0\,, \tag{8}$$

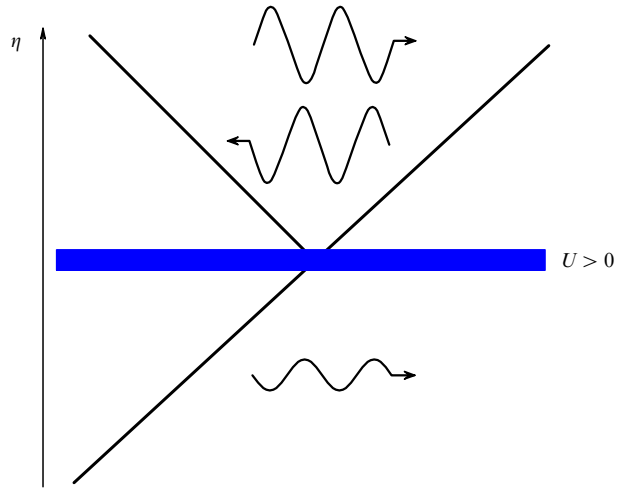

Figure 2. Illustration of the solution of Eqn (8) in the scattering problem.

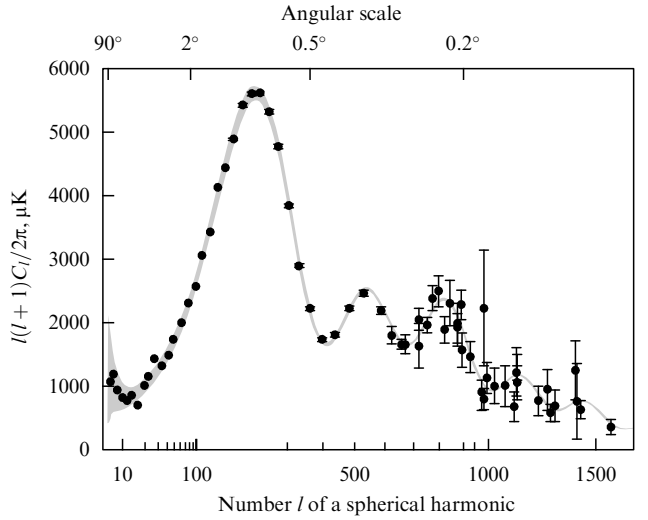

Figure 3. Manifestation of sound modulation of CMB anisotropy spectrum. [According to the data of the WMAP, ACBAR (Arcminute Cosmology Bolometer Array Receiver), BOOMERANG (Balloon Observations Of Millimetric Extragalactic Radiation ANd Geophysics), CBI (Cosmic Background Imager), and VSA (Very Small Array) experiments.]

where

$$\bar{q} \equiv \alpha q\,, \qquad U \equiv \frac{\alpha''}{\alpha}\,. \tag{9}$$

The solution to Eqn (8) has two asymptotic branches: the adiabatic branch ($\omega^2 > U$), where an oscillator is freely oscillates and its excitation amplitude decays ($|q| \sim (\alpha\sqrt{\beta}\,)^{-1}$), and the parametric branch ($\omega^2 < U$), where the field q is frozen ($q \to \text{const}$). The latter condition means, from the viewpoint of quantum-field theory, parametric production of a pair of particles from a state with elementary excitation (Fig. 2).

Quantitatively, the spectra of the produced perturbations depend on the initial state of the oscillators:

$$T \equiv 2\langle q_T^2\rangle\,, \qquad S \equiv \langle q_S^2\rangle\,, \tag{10}$$

with the factor '2' in the expression for the tensor mode accounting for two polarizations of gravitational waves. The state $\langle\,\rangle$ is assumed to be the ground state, i.e., it corresponds to the minimum level of initial excitation of the oscillators. This constitutes the main hypothesis for the Big Bang theory. In the presence of an adiabatic zone, the ground (vacuum) state of elementary excitations is uniquely determining [7].

Thus, assuming that the function U increases with time and that $\beta \sim 1$, we arrive at a universally general result for the spectra $T(k)$ and $S(k)$:

$$T \approx \frac{(1-\gamma/2)H^2}{M_{\rm P}^2}\,, \qquad \frac{T}{S} \approx 4\gamma\,, \tag{11}$$

where $k = \sqrt{U} \approx aH$, and $M_{\rm P} \equiv G^{-1/2}$ is the Planck mass. From formulas (11) we see that in theory the mode T is never discriminated in relation to mode S. Everything depends on the value of the factor γ at the epoch of excitation generation.

From the observed fact that the T mode is small in our Universe [see Eqn (1) in Section 2], we obtain the upper bounds on the energy scale of the Big Bang and on the parameter γ in the early Universe:

$$H < 10^{13}\ \text{GeV}\,, \qquad \gamma < 0.05\,. \tag{12}$$

The second condition means that the Big Bang was inflationary ($\gamma < 1$).

Thus, we possess an important phase information, namely, that the fields are created in a certain phase, and only the growing branch of the perturbations is parametrically amplified. Let us explain this fact on the example of scattering problem, assuming that $U = 0$ in the *initial* (adiabatic) and *final* (radiation-dominated, $a \propto \eta$) stages of evolution (see Fig. 2).

For each of the above-mentioned asymptotics, the general solution is written in the form

$$\bar{q} = C_1 \sin\omega\eta + C_2 \cos\omega\eta\,, \tag{13}$$

where the operators $C_{1,2}$ specify the amplitudes of the 'growing' and 'decaying' evolution branches. In the vacuum state, the field's initial temporal phase is arbitrary: $\langle|C_1^{(\rm in)}|\rangle = \langle|C_2^{(\rm in)}|\rangle$. However, after solving the evolution equations it turns out that at the radiation-dominated stage only the growing branch of acoustic perturbations is created: $\langle|C_1^{(\rm out)}|\rangle \gg \langle|C_2^{(\rm out)}|\rangle$. By the instant of time when radiation decouples from matter in the recombination epoch, the radiation spectrum is modulated with a phase $k = n\pi\sqrt{3}/\eta_{\rm rec}$, where n is a natural number.

It is precisely these acoustic vibrations that are observed in the spectra of the CMB anisotropy (see Fig. 3, where the high peak corresponds to $n = 1$) and the density perturbations, which are proofs of the quantum-gravitational origin of the S mode. In the density perturbations spectrum, the acoustic modulation is suppressed by the smallness of the fraction of baryons in the total budget of matter, which makes it possible to find this fraction irrespective of other cosmological tests. The scale of baryonic oscillations is used as a standard ruler for determining the important parameters of the Universe. In view of this, it must be noted that the acuteness of the problem of degeneracy of cosmological parameters in the observational data, which for many years impeded the building up of the real model of the Universe, has finally been resolved thanks to the

numerous independent and complementary observational tests.

Summarizing, we can ascertain that the problem of formation of the initial cosmological perturbations and the large-scale structure of the Universe has been solved (at least in principle). The theory of the quantum-gravitational origin of perturbations in the early Universe will receive further confirmation after the T mode is discovered, which may happen very soon. For instance, the simplest model of the Big Bang (power-law inflation on a massive scalar field) predicts the value of the T-mode amplitude only five times smaller than the S-mode amplitude [8]. Modern instruments and techniques make it possible to detect such weak signals in the CMB data on the anisotropy and polarization.

4. The dark side of matter

There are several hypotheses concerning the origin of matter, but none of them has been confirmed. We have also straightforward observational indications that the dark matter mystery is closely related to the baryon asymmetry in the Universe. However, today there is no widely accepted theory of the origin of both baryon asymmetry and dark matter.

Where is dark matter?

We know that the luminous component of matter is observed in the form of stars assembled into galaxies of various masses and in the form of X-ray gas in clusters. However, the larger part of ordinary matter (up to 90%) is in the form of rarefied intergalactic gas with a temperature of several electron-volts and in the form of MACHOs (Massive Compact Halo Object), the compact remnants from the star evolution and small-mass objects. Since these structures usually possess low luminosity, they are known as 'dark baryons'.

Several collaborations (MACHO, EROS, and some others) have investigated the amount and distribution of compact dark objects in the halo of our Galaxy by studying microlensing events. As a result of joint analysis, an important bound was obtained: no more than 20% of the entire halo mass is in MACHOs in the range from the mass of the Moon to stellar masses (Fig. 4). The remainder of the dark mass of the halo consists of particles of unknown origin.

Where else can nonbaryonic dark matter hide?

The development of high technologies in 20th-century observational astronomy gave a clear answer to this question;

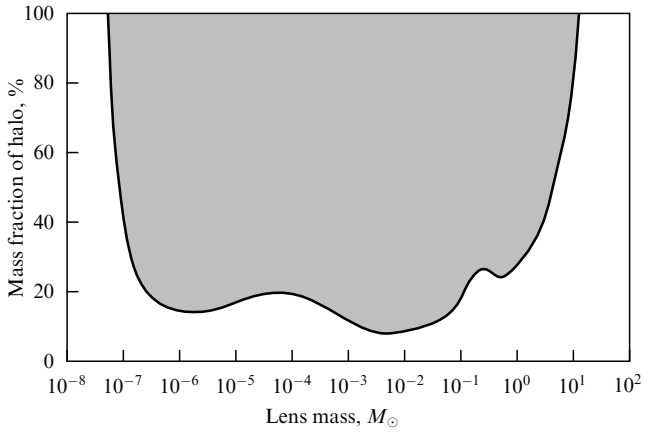

Figure 4. Upper bound on the mass fraction of the Galaxy halo in MACHOs according to EROS (Expérience pour la Recherche d'Objets Sombres) experiment.

Table 2. Candidates for particles of nonbaryonic dark matter.

Candidate	Mass
Gravitons	10^{-21} eV
Axions	10^{-5} eV
Sterile neutrinos	10 keV
Mirror matter	1 GeV
Massive particles	100 GeV
Supermassive particles	10^{13} GeV
Monopoles and defects	10^{19} GeV
Primordial black holes	$(10^{-16} - 10^{-7})M_\odot$

namely, nonbaryonic dark matter is located in gravitationally bound systems (halos). The particles of dark matter are nonrelativistic and weakly interacting; they do not dissipate like baryons. Baryons radiationally cool off, precipitate, and accumulate in halo centers, achieving rotational equilibrium. Dark matter remains distributed around the visible matter of galaxies with a characteristic scale of about 200 kpc. For instance, in the Local Group, which includes the Andromeda Nebula and the Milky Way, more than half of all dark matter is concentrated in these two big galaxies.

Particles with the required properties are absent in the Standard Model of elementary particle physics. An important parameter that cannot be determined from observations due to the Equivalence principle is the mass of particles. Within the scope of various extensions of the Standard Model there are several candidates for dark matter particles. The main candidates are listed in Table 2 in ascending order of their rest masses.

The main hypothesis for massive particles, the neutralino hypothesis, is related to minimal supersymmetry. The hypothesis could be verified with the Large Hadron Collider at CERN, which should become operational in 2008. The expected mass of such particles is about 100 GeV, and their number density in our Galaxy is one particle per volume of a tea cup.

The search for dark-matter particles continues at many laboratories all over the world. What is interesting is that the neutralino hypothesis allows independent verification in underground experiments in elastic scattering and by using indirect data on the annihilation of neutralinos in the Galaxy. So far there has been only one positive response in one of the underground detectors of the DAMA (DArk MAtter) project, where for several years researchers have recorded a signal of unknown origin of the 'summer–winter' type. As yet, however, the ranges of masses and cross sections related to this experiment have not been confirmed in other experiments, which raises doubts concerning the reliability and significance of such a result.

An important property of neutralinos is the possibility of observing them indirectly by the annihilation flux in the gamma band. In the process of hierarchic clustering, such particles could have formed minihalos with a characteristic size on the order of the solar system dimension and a mass of about that of the Earth, with the remains still surviving today. It is highly probable that the Earth itself is inside such minihalos, where the particle number density increases by a factor of several dozen. This increases the probability of detecting, both directly and indirectly, dark matter in our Galaxy. The fact that there are so many different methods of searching for dark matter raises hopes, and makes it possible to believe, that the riddle of the physical nature of dark matter will soon be solved.

5. At the verge of the new physics

In our times it has become possible to independently determine the properties of the early Universe and the late Universe from observational astronomical data. We understand how the initial cosmological density perturbations emerged and how the modern structure of the Universe has developed from them. We know the values of the main cosmological parameters lying at the basement of the Standard Model of the Universe, the model has no visible rivals. However, the fundamental problems of the origin of the Big Bang and of the main components of matter still remain unresolved.

Determining the tensor mode of cosmological perturbations from observational data is the key issue in building up the model of the early Universe. Here, we are dealing with an accurate prediction of the theory that has been verified in the case of the S mode and can be experimentally verified for the T mode in the near future.

Theoretical physics, which has proposed many avenues of research and methods of searching for particles of dark matter, has exhausted itself. Now, it is experiment's turn. The current situation resembles the one just before the great discoveries: quarks, W- and Z-bosons, neutrino oscillations, and the anisotropy and polarization of CMB.

There is one question, however, that goes beyond the present report: Why is nature so benevolent and why does it open up its secrets to us?

The present work was made possible by partial support of the Russian Foundation for Basic Research (grants Nos 07-02-00886 and 05-02-16302).

References

1. Grib A A, Mamaev S G, Mostepanenko V M *Kvantovye Effekty v Intensivnykh Vneshnikh Polyakh: Metody i Rezul'taty, Ne Svyazannye s Teoriei Vozmushchenii* (Quantum Effects in Intense External Fields: Methods and Results Unrelated to Perturbation Theory) (Moscow: Atomizdat, 1980); see also by the same authors: *Vacuum Quantum Effects in Strong Fields* (St.-Petersburg: Friedmann Laboratory Publ., 1994)
2. Zel'dovich Ya B, Starobinskii A A *Zh. Eksp. Teor. Fiz.* **61** 2161 (1971) [*Sov. Phys. JETP* **34** 1159 (1972)]
3. Grishchuk L P *Zh. Eksp. Teor. Fiz.* **67** 825 (1974) [*Sov. Phys. JETP* **40** 409 (1975)]
4. Lukash V N *Zh. Eksp. Teor. Fiz.* **79** 1601 (1980) [*Sov. Phys. JETP* **52** 807 (1980)]
5. Lukash V N, astro-ph/9910009
6. Strokov V N *Astron. Zh.* **84** 483 (2007) [*Astron. Rep.* **51** 431 (2007)]
7. Lukash V N *Usp. Fiz. Nauk* **176** 113 (2006) [*Phys. Usp.* **49** 103 (2006)]
8. Lukash V N, Mikheeva E V *Int. J. Mod. Phys. A* **15** 3783 (2000)